

**KINETIC AND RAPID SCAN SPECTROPHOTOMETRIC  
STUDIES OF THE OLIGOMERIZATION OF ETHENE  
AND PROPENE USING THE CATALYTIC SYSTEM  
[Ni(sacsac)P(n-butyl)<sub>3</sub>Cl]/AlEt<sub>2</sub>Cl**

MARTIN P. C. MASON, JOHN I. SACHINIDIS  
and PETER A. TREGLOAN\*

School of Chemistry, The University of Melbourne, Parkville, Victoria, 3052, Australia

and

ANTHONY F. MASTERS\*

School of Chemistry, University of Sydney, Sydney, New South Wales, 2006, Australia

(Received 3 March 1994; accepted 12 July 1994)

**Abstract**—Rate data and *in situ* UV–vis spectra of the [Ni(sacsac)P(n-butyl)<sub>3</sub>Cl]/AlEt<sub>2</sub>Cl catalytic system for the oligomerization of ethene and propene are reported. The general form of the rate profile for the consumption of alkene feedstock during the establishment and maintenance of the catalytic cycle depends quite dramatically on the dryness of the alkene and the sequence of activation of the nickel complex by aluminum alkyl. A number of UV–vis spectral features of the precursor and active species formed can be identified. In particular, the appearance of an absorbance peak at around 420 nm can be used to anticipate the loss of catalytic activity. The process leading to formation of the Ni<sup>II</sup> species responsible for the 420 nm absorption can be reversed by addition of excess AlEt<sub>2</sub>Cl.

The use of Ziegler type catalysts in producing higher alkenes and specialty chemicals from lower alkenes is widespread and a large number of nickel-based catalytic systems has been reported.<sup>1–9</sup> The most notable industrial applications are the Shell Higher Olefin Process (SHOP)<sup>1,10,11</sup> and the Dimersol processes.<sup>12–14</sup>

The catalytic system in this study consists of a *d*<sup>8</sup> nickel(II) square-planar complex [Ni(sacsac)PR<sub>3</sub>Cl], where sacsac = pentane-2,4-dithionate and R = n-butyl, activated by diethylaluminium chloride (AlEt<sub>2</sub>Cl), which exists as a labile dimer in solution. This system has previously been reported as one of the most active and stable catalytic systems for the oligomerization of alkenes.<sup>15</sup> The major operational advantage over existing commercial

processes is the exceptionally high catalytic activity at atmospheric pressure and ambient temperatures.

The most widely accepted mechanism for transition metal catalysed oligomerization is a chain process initiated by alkene coordination involving a nickel hydride or nickel alkyl species, followed by migratory insertion.<sup>4</sup> Tertiary phosphines, either coordinated in the original nickel complex or added as free phosphine, are thought to tailor the product distribution.<sup>6</sup>

To gain more insight into the nature of the active catalytic species, a technique for measuring UV–vis spectral changes during oligomerization has been developed. Very few Ziegler type catalytic systems have been studied by UV–vis spectral measurements, with the main ones being those reported by Onsager *et al.*<sup>16</sup> and Smidt *et al.*<sup>17</sup> The [Ni(sacsac)P(n-butyl)<sub>3</sub>Cl] precursor has a well defined absorption maximum at 328 nm ( $\epsilon$  ca 14,000 dm<sup>3</sup> cm<sup>-1</sup> mol<sup>-1</sup>), so, in this work, simultaneous UV–

\*Authors to whom correspondence should be addressed.

vis spectra and rate measurements were monitored and collated, in contrast to our previous studies,<sup>15</sup> which have only measured kinetic data derived from the consumption of alkene.

## EXPERIMENTAL

### Materials

[Ni(sacsac)P(n-butyl)<sub>3</sub>Cl] was synthesized according to the published method.<sup>18</sup> Diethylaluminium chloride (Merck/Aldrich, 97%) was used without further purification to prepare a 0.41 M stock solution in chlorobenzene. Chlorobenzene (B.D.H., LR) was refluxed in a dry nitrogen atmosphere over calcium hydride (B.D.H., LR) for a minimum of 1 h prior to use. Solvent prepared in this manner was analysed for water content by Karl Fischer coulometry and found to contain *ca* 15 ppm H<sub>2</sub>O. The alkene substrates, ethene (Matheson, C.P., 99.0% min.) and propene (C.I.G., C.P., 99.5% min.), were used as received.

All manipulations were performed in a nitrogen atmosphere using standard manifold techniques<sup>19</sup> or in a dry box. All glassware was dried in an oven at 110°C for at least 1 h before use.

### Oligomerization equipment

The oligomerization apparatus used is described below and illustrated in Fig. 1. Swagelok fittings and 1/4" copper and stainless steel tubing were used to connect the various components. The reaction vessel could be connected to a vacuum line for drying, or to the feed line for an oligomerization experiment via a three-way valve (Whitey B-42XS4).

*Reaction vessel.* The cylindrical reaction vessel, illustrated in Fig. 2, was constructed of stainless steel and closed with a flat circular plate, secured

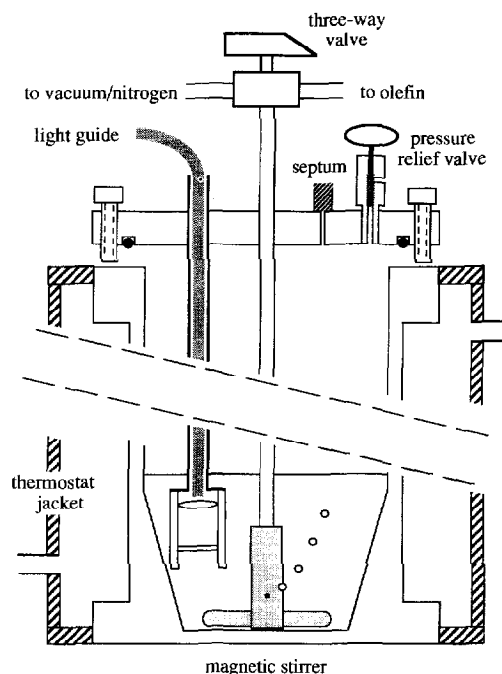


Fig. 2. Cross-section of experimental arrangement in oligomerization vessel.

by hex-key screws and sealed by a Viton O-ring. The vessel was enclosed by a cylindrical PVC thermostating jacket. An ethanol-water mixture ( $5.0 \pm 0.5^\circ\text{C}$ ) was circulated through the jacket from a thermostat bath (Cole-Parmer). The lid of the vessel was fitted with several attachments: a three-way valve for connection to feed or vacuum line, a septum for the addition of reagents, a UV-vis spectrophotometric probe and a relief valve (Nupro, RL3) set at 10 atm. The three-way tap was connected to 1/4" stainless steel tubing which ran axially down the vessel and acted as a shaft for the Teflon-coated magnetic spindle used to stir the solution. The spindle was perforated at several points to allow the gas into the reaction mixture.

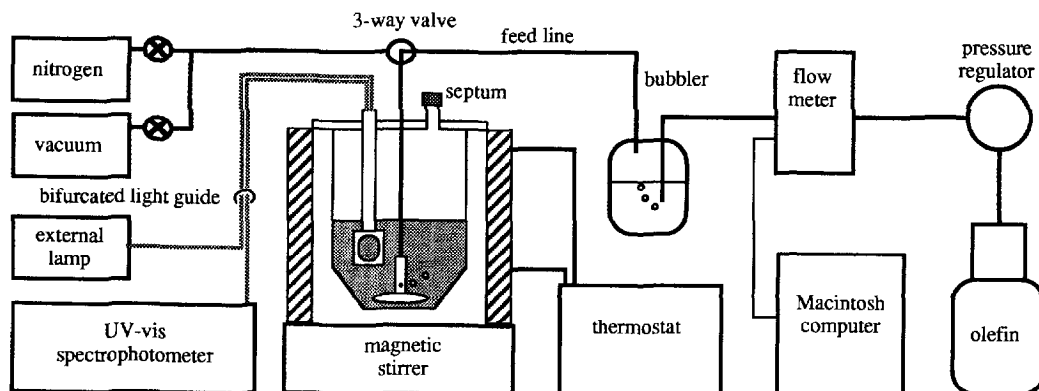


Fig. 1. Experimental set-up for oligomerization kinetics of propene or ethene.

The UV-vis spectrophotometric probe was attached to a stainless steel tube, containing a quartz fibre light guide and mounted through the lid; it is illustrated in more detail in Fig. 3. The probe consisted of a polished stainless steel mirror held opposite a fused silica collimating lens (Oriel 77644) by an open frame which enabled the reaction mixture to circulate freely. The lens mount was sealed using a Viton O-ring.

*Flow-meter measurements.* As described by Masters *et al.*,<sup>15</sup> the reaction kinetics can be followed by monitoring the consumption of substrate by mass difference using a top loading balance. However, this method is impractical for ethene, so the rate of consumption was measured using a mass flow meter (Porter Instruments Co. 100F) which produces a voltage proportional to flow rate. The meter was calibrated by the manufacturer. The output from the flow-meter was connected to a Forth laboratory micro-processor/controller<sup>20</sup> for signal conversion. The digitized signal was transferred to an Apple Macintosh computer for data storage and manipulation.

*UV-vis spectrophotometry.* UV-vis spectra were recorded using a Hewlett-Packard 8452A diode array UV-vis spectrophotometer connected to the reaction vessel via a 1 m bifurcated light guide (Dolan Jenner, UV grade). One of the bifurcated arms was used to direct incident light to the probe, the other was used to return the transmitted light to the detector. The intensity of the spectrophotometer's internal lamp was not high enough in the UV region for satisfactory transmission through the light guide, so a xenon arc lamp (Oriel 75W with Oriel Power Supply 68806) was used. Spectra obtained by this method were comparable to spectra recorded in a standard quartz cell down to 280 nm, but below this wavelength the spectra became very noisy and irreproducible. The effective path length of the probe was adjusted to be 10 mm.

Figure 4 shows the spectrum of  $[\text{Ni}(\text{sacsac})\text{P}(\text{n-butyl})_3\text{Cl}]$  in chlorobenzene recorded in the reaction vessel ( $[\text{Ni}] = 8.6 \times 10^{-5} \text{ M}$ ). The characteristic  $\lambda_{\text{max}}$  at 328 nm, and other minor peaks are clearly

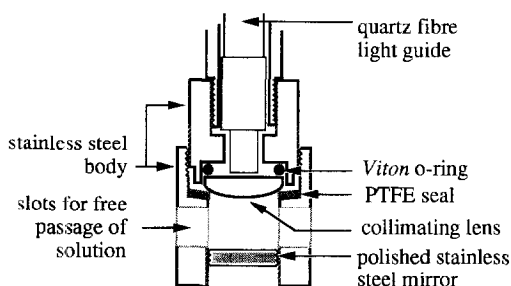


Fig. 3. Detail of UV-vis spectrophotometric probe cell.

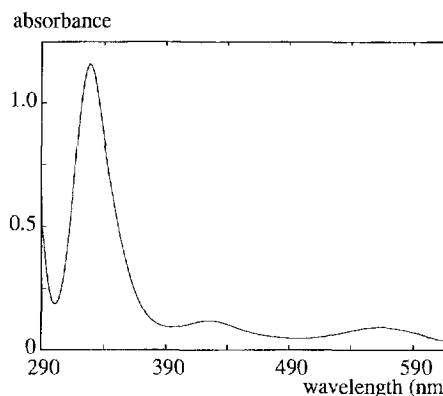


Fig. 4. UV-vis spectrum of  $[\text{Ni}(\text{sacsac})\text{P}(\text{n-butyl})_3\text{Cl}]$  in chlorobenzene recorded in the reaction vessel using the UV-vis spectrophotometric probe,  $[\text{Ni}] = 8.6 \times 10^{-5} \text{ M}$ .

defined. Spectra of this clarity were obtainable routinely using the quartz fibre optics system.

#### Procedure

The reaction vessel was assembled and dried under vacuum for at least 2 h. It was put through two nitrogen/vacuum cycles before being charged with alkene gas. The vessel was then thermostatted and the solvent (chlorobenzene, 150 cm<sup>3</sup>) injected and allowed to saturate with alkene. A spectrophotometric blank was recorded and the flow monitoring was commenced. An aliquot of the  $\text{AlEt}_2\text{Cl}$  co-catalyst solution was normally injected first, followed within 2 min by the  $[\text{Ni}(\text{sacsac})\text{P}(\text{n-butyl})_3\text{Cl}]$  solution, to initiate the reaction.

## RESULTS

Mass-flow data and UV-vis spectral data were collected simultaneously. The details of the rate profiles obtained varied according to the order of addition of catalyst and co-catalyst. Since water is known to affect the operation of the catalytic system,<sup>21</sup> some experiments were carried out where the alkene was bubbled through an  $\text{AlEt}_2\text{Cl}$  solution to dry the substrate. It should be noted that as the oligomerization proceeds, the build up of products dilutes the reaction mixture and may affect the observed kinetics. At this stage no attempt has been made to correct for this when analysing the kinetic behaviour.

#### Propene rate profiles

*AlEt<sub>2</sub>Cl added before  $[\text{Ni}(\text{sacsac})\text{P}(\text{n-butyl})_3\text{Cl}]$  using dried substrate.* The simplest rate profile to consider is that obtained when oligomerizing dried

propene. Figure 5a shows a typical profile, where  $\text{AlEt}_2\text{Cl}$  solution was injected to give an initial  $\text{AlEt}_2\text{Cl}$  concentration,  $[\text{Al}]_0$ , of  $5.88 \times 10^{-3}$  M, followed by injection of  $[\text{Ni}(\text{sacsac})\text{P}(\text{n-butyl})_3\text{Cl}]$  solution to give an initial nickel concentration,  $[\text{Ni}]_0$ , of  $8.6 \times 10^{-5}$  M (i.e.  $[\text{Ni}]_0 : [\text{Al}]_0 = 1 : 68$ ).

Profiles from this type of experiment can be described in terms of three stages. A rapid activation occurs within the first 5 min, with the rate reaching a maximum. After this, the rate decreases to a constant value which is maintained for a time, typically 1–4 h, proportional to the nickel concentration. The rate then decreases to zero over the next 1–2 h.

$[\text{Ni}(\text{sacsac})\text{P}(\text{n-butyl})_3\text{Cl}]$  added before  $\text{AlEt}_2\text{Cl}$  using dried substrate. Experiments reversing the order of addition of the catalyst and co-catalyst gave a dramatically different reaction profile. The first 20 min of the experiment in Fig. 5b, where  $[\text{Ni}]_0$  and  $[\text{Al}]_0$  were identical to the experiment in Fig. 5a but where the order of addition of nickel complex and  $\text{AlEt}_2\text{Cl}$  was reversed, shows that the

initial periods of activation were very similar; however, after attaining a maximum, the rate rapidly decreased to zero in the experiment where the nickel complex was added first.

If a larger aliquot of  $\text{AlEt}_2\text{Cl}$  was used, then the catalytic activity could be maintained for several hours. Figure 5c shows such an experiment in which the  $[\text{Ni}(\text{sacsac})\text{P}(\text{n-butyl})_3\text{Cl}]$  was added to give  $[\text{Ni}]_0 = 7.61 \times 10^{-5}$  M, followed by  $\text{AlEt}_2\text{Cl}$  solution to give  $[\text{Al}]_0 = 1.08 \times 10^{-2}$  M ( $[\text{Ni}]_0 : [\text{Al}]_0 = 1 : 141$ ).

*Rate profiles using undried substrate.* The order of addition of catalyst and co-catalyst for experiments using undried substrate did not appear to have any significant effect on the shape of the profile. With either order of addition, an initial rapid activation period was observed after which the rate rapidly decreased to zero. This is shown in the initial 25 min of Fig. 6, where  $[\text{Ni}]_0 = 2.14 \times 10^{-4}$  and  $[\text{Al}]_0 = 6.34 \times 10^{-3}$  M ( $[\text{Ni}]_0 : [\text{Al}]_0 = 1 : 30$ ).

*Reactivation of the catalytic system.* After the initial loss of activity, the system could be reactivated by a further addition of  $\text{AlEt}_2\text{Cl}$ . Whether the substrate was dried or undried this resulted in a similar profile, showing two maxima, one at the beginning and one at the end of the reactivation phase. This is shown in Fig. 5b between 120 and 340 min and in Fig. 6 between 30 and 120 min. Addition of  $[\text{Ni}(\text{sacsac})\text{P}(\text{n-butyl})_3\text{Cl}]$  after the first loss of activity, however, did not reactivate the system. This suggests that this loss of catalytic activity is due to the depletion of co-catalyst from the mixture.

After the second loss of activity, addition of a third aliquot of  $\text{AlEt}_2\text{Cl}$  did not reestablish catalysis; however, addition of  $[\text{Ni}(\text{sacsac})\text{P}(\text{n-butyl})_3\text{Cl}]$  did. An example of this is shown in Fig. 6 at 150

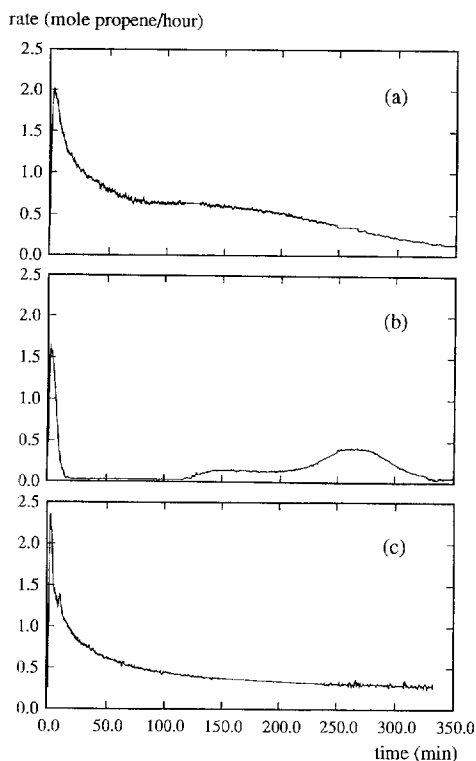


Fig. 5. Rate profiles for dried propene changing the order of addition of reagents. (a)  $\text{AlEt}_2\text{Cl}$  added before  $[\text{Ni}(\text{sacsac})\text{P}(\text{n-butyl})_3\text{Cl}]$ ,  $[\text{Ni}]_0 = 8.6 \times 10^{-5}$  and  $[\text{Al}]_0 = 5.88 \times 10^{-3}$  M. (b)  $[\text{Ni}(\text{sacsac})\text{P}(\text{n-butyl})_3\text{Cl}]$  added before  $\text{AlEt}_2\text{Cl}$ ,  $[\text{Ni}]_0 = 8.6 \times 10^{-5}$  and  $[\text{Al}]_0 = 5.6 \times 10^{-3}$  M. Reactivated with  $\text{AlEt}_2\text{Cl}$  at 120 min. (c) Large amount of  $\text{AlEt}_2\text{Cl}$  added after  $\text{Ni}(\text{sacsac})\text{P}(\text{n-butyl})_3\text{Cl}$ ,  $[\text{Ni}]_0 = 7.61 \times 10^{-5}$  and  $[\text{Al}]_0 = 1.08 \times 10^{-2}$  M.

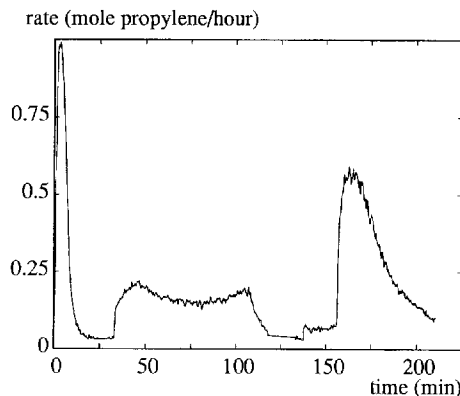


Fig. 6. Rate profile for undried propene.  $[\text{Ni}]_0 = 2.14 \times 10^{-4}$  and  $[\text{Al}]_0 = 6.34 \times 10^{-3}$  M. Reactivated with  $\text{AlEt}_2\text{Cl}$  at 65 min and again with  $\text{AlEt}_2\text{Cl}$  at 140 min and then  $[\text{Ni}(\text{sacsac})\text{P}(\text{n-butyl})_3\text{Cl}]$  at 155 min.

min. This suggests that the depletion of active nickel causes the second deactivation.

#### Ethene rate profiles

Rate profiles for the oligomerization of ethene were similar to those described above, but the reaction occurred much more rapidly. Although the ethene experiments were shorter lived than those using propene, the number of moles of gas converted per mole of catalyst was similar. However, it was observed that for ethene experiments the maximum oligomerization rate was limited by the speed of stirring of the solution. This implies that in our experimental arrangement the diffusion of the substrate is rate limiting for ethene, in contrast to propene where stirring changes had no such effect.

#### Spectral changes

*UV-vis spectral changes using propene.* In the initial stages of reaction there were no observed differences in spectral changes between experiments using dried or undried propene. Typical changes occurring during the first 60 s of an oligomerization experiment are shown in Fig. 7, where the reaction was carried out using dried propene, with  $[Ni]_0 = 8.6 \times 10^{-5}$  M and  $[Al]_0 = 5.88 \times 10^{-3}$  M (spectra were recorded at 10 s intervals;  $[Ni]_0 : [Al]_0 = 1 : 68$ ). The broken line shows the absorbance of the precursor measured before the addition of co-catalyst. These data were recorded during the early stages of the experiment shown in Fig. 5b.

Upon addition of co-catalyst, a very rapid initial

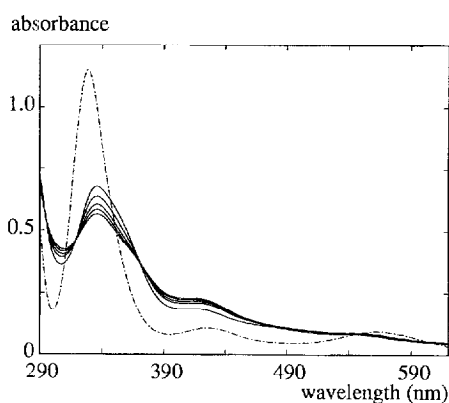


Fig. 7. UV-vis spectra of catalytic mixture during oligomerization of propene recorded in the reaction vessel using the UV-vis spectrophotometric probe at 10 s intervals. Broken line shows the absorbance measured before the addition of co-catalyst.

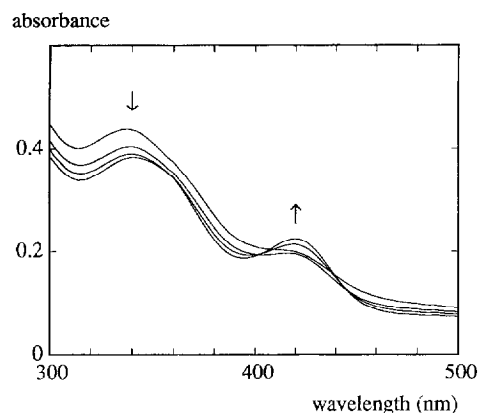


Fig. 8. UV-vis spectra of catalytic mixture during oligomerization as rate decreases, recorded at 100 s intervals.

process was observed leading to a new  $\lambda_{max}$  at 336 nm. This was followed by a slower conversion, with isosbestic points noted at 319 and 372 nm. As the reaction proceeded further, the absorbance decreased over all wavelengths. This is consistent with a dilution of the absorbing species, due to an increase in solution volume as the liquid hexene products form.

Towards the end of catalytic activity, corresponding to around 10 min in Fig. 6, while the absorbance decreased at most wavelengths, a peak appeared at 420 nm. Figure 8 shows the appearance of this peak at 420 nm as catalytic activity was being lost. When the reaction was reactivated by the addition of  $AlEt_2Cl$ , the 420 nm peak disappeared. Figure 9 overlays absorbance and rate vs time data for a run with undried substrate and dramatically illustrates the inverse correlation between catalytic activity and changes in absorbance around 420 nm.

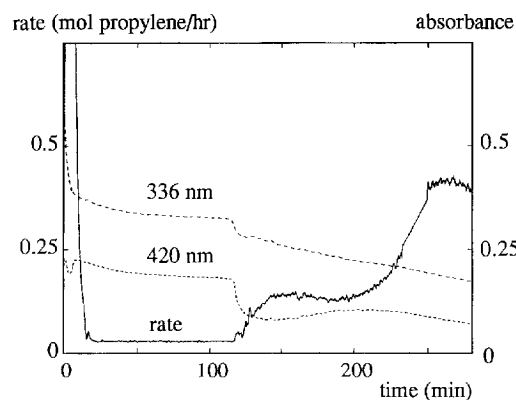


Fig. 9. Comparison of rate and absorbance profiles for dried propene;  $[Ni(sacsac)P(n-butyl)_3Cl]$  added before  $AlEt_2Cl$ . Solid line shows rate of propene ( $mol\ h^{-1}$ ), broken lines show absorbance at 336 and 420 nm (as labelled).

The absorbance changes at 336 nm are also shown for comparison. During the period of no catalytic activity between 20 and 120 min, the decrease in absorbance at both wavelengths is possibly due to slow precipitation of the absorbing species.

Of the two ways in which catalytic activity can be lost, depletion of  $\text{AlEt}_2\text{Cl}$  or loss of active nickel from the reaction cycle, the appearance of the peak around 420 nm only seems to be associated with the depletion of  $\text{AlEt}_2\text{Cl}$  and the loss of this absorption is associated with the addition of  $\text{AlEt}_2\text{Cl}$ .

*UV-vis spectral changes using ethene.* The general spectral characteristics observed during ethene oligomerization reactions exhibit similar features to propene oligomerization. The specific wavelengths of maximum absorbance after mixing and the isosbestic points differ slightly from those observed for the propene experiments.

## DISCUSSION

The rate of alkene consumption and the spectral changes were monitored simultaneously. The rate profiles obtained depend on

- (i) the order of addition of catalytic reagents,
- (ii) whether the alkene was dried or not, and
- (iii) the alkene used.

Rate profiles using dried propene, with  $\text{AlEt}_2\text{Cl}$  added before  $[\text{Ni}(\text{sacsac})\text{P}(\text{n-butyl})_3\text{Cl}]$ , were the simplest and exhibited the longest period of activity, typically running for 4–6 h. These profiles were similar in shape to those obtained by Onsager *et al.*<sup>16</sup> using a nickel-based Ziegler type catalytic system. Reversing the order of addition resulted in shortening of the initial catalytic activity to less than 10 min. Addition of further  $\text{AlEt}_2\text{Cl}$  reactivated the system. The magnitude of the resulting activity depended on the amount of  $\text{AlEt}_2\text{Cl}$  added. Once this re-induced catalytic activity had stopped, addition of both reagents was required to reactivate the system.

We have reported previously<sup>15</sup> that the rate during a catalysis run often increases significantly immediately before termination of the oligomerization reaction. In the experiments reported here, this is most apparent in Fig. 5b. One explanation is the existence of two catalytic centres, one formed on mixing and the other building up as the first decays, then itself being deactivated. Kinetic analysis of the dimerization of butene using this catalytic system has also suggested the operation of two catalytic species in the reacting solution.<sup>22</sup>

Experiments conducted with undried propene resulted in behaviour similar to that for dried substrate where  $[\text{Ni}(\text{sacsac})\text{P}(\text{n-butyl})_3\text{Cl}]$  was added

before  $\text{AlEt}_2\text{Cl}$ . The period of activity was always shorter with undried propene.

From these experimental observations it appears that the  $\text{AlEt}_2\text{Cl}$  species has a dual role. Initially it reacts with the nickel species to form the active catalyst and, secondly, as illustrated by the extended catalytic lifetimes using dried substrate, where bubbling the feedstock alkene through a solution of alkylaluminium halide has been effective in increasing the yield by over a factor of 10,<sup>15</sup> the  $\text{AlEt}_2\text{Cl}$  acts to protect the active species from poisons such as water.

From our experiments, it appears that even the initial activation in the catalytic cycle is a multi-step process. The stages and changes occurring in the activation and cycle are summarized in the schematic in Fig. 10. The absorbance maximum at 328 nm, corresponding to the initial nickel complex (stage A), is converted to a maximum at 336 nm (stage B), which, in a process (or processes) which generates isosbestic points at around 320 and 370 nm, changes to an absorbance maximum at 346 nm (stage C).

The first step, A to B, is a sub-second conversion to one or more species followed by a slower conversion to new species at stage C. The conversion from stages A to B may be observed using spectrophotometric stopped flow experiments; these are currently underway. The presence of isosbestic points in the conversion from stages B to C suggest that this is a simple 1:1 reaction. It is after the

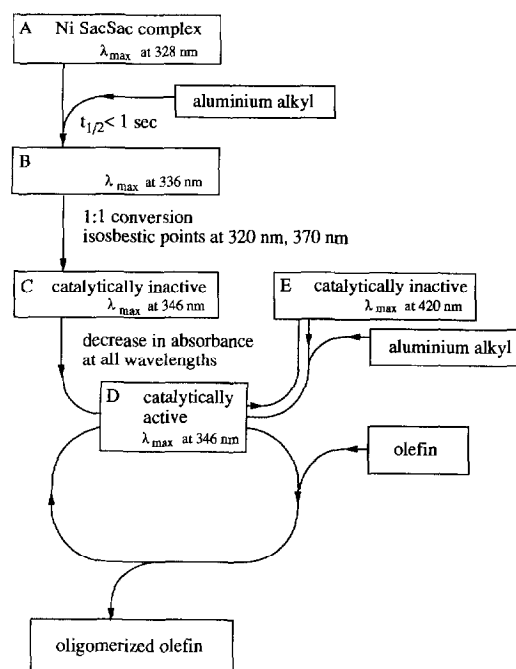


Fig. 10. Schematic representation of reaction sequence and features of spectral changes.

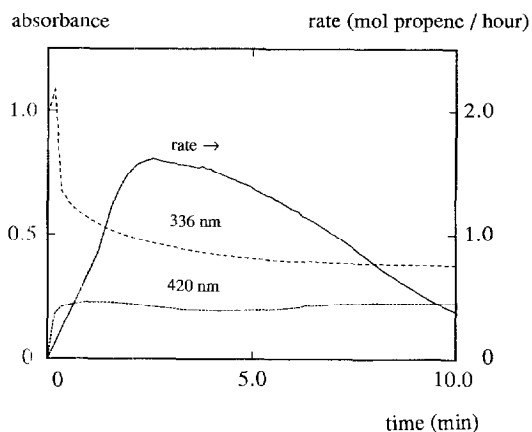


Fig. 11. Expansion of initial 10 min in Fig. 9, showing the rate (solid line) reaching a maximum after the formation of species at reaction stage 'C'.

formation of the species at stage C that the maximum rate of oligomerization is achieved. Indeed, as is illustrated in Fig. 11, the maximum rate of activity does not occur until *ca* 3 min after the formation of these species at stage C, indicated by the rapid decrease in absorbance at 336 nm (corresponding to the shift in band shape to give a maximum at 346 nm). There is a significant decrease in absorbance at the end of the activation period but the spectral characteristics of the active species at D are similar to those of the species at C.

Regardless of the initial reaction conditions, the sequence from the initial species at A to those formed at B and converted to C was always observed. The appearance of the band at 420 nm was found to be characteristic of reversible loss of catalytic activity under all oligomerization experimental conditions. This was shown to correspond to the loss of excess  $\text{AlEt}_2\text{Cl}$  from the reaction mixture, as it could be reversed by the addition of fresh  $\text{AlEt}_2\text{Cl}$ , and would appear to be most consistent with the protective role of  $\text{AlEt}_2\text{Cl}$  referred to earlier. The most obvious protective role is against water interfering with the operation of the catalyst and this therefore appears to be reversible. We are currently carrying out further kinetic and spectroscopic, including NMR, studies of this system to characterize the nature of the precursor species involved.

*Acknowledgement*—The support of the Australian Research Council is gratefully acknowledged.

## REFERENCES

1. W. Keim, *Angew. Chem., Int. Edn Engl.* 1990, **29**, 235.
2. C. T. O'Connor and M. Kojima *Catal. Today* 1990, **6**, 329.
3. S. Muthukumar Pillai, M. Ravindranathan and S. Sivaram, *Chem. Rev.* 1986, **86**, 353.
4. O. T. Onsager and J. E. Johansen, in *The Chemistry of the Metal-Carbon Bond* (Edited by F. R. Hartley and S. Patai), Vol. 3, p. 205. Wiley, Brisbane (1985).
5. W. Keim, A. Behr and M. Roper, in *Comprehensive Organometallic Chemistry* (Edited by G. Wilkinson, F. G. A. Stone and E. W. Abel), Vol. 8, p. 371. Pergamon Press, Oxford (1982).
6. B. Bogdanovic, *Adv. Organomet. Chem.* 1979, **17**, 105.
7. V. Sh. Fel'dblyum and N. V. Obeshchlova, *Russ. Chem. Rev.* 1968, **37**, 789.
8. A. M. Al-Jarallah, J. A. Anabtawi, M. A. B. Siddiqui, A. M. Aitani and A. W. Al-Sa'Doun, *Catal. Today* 1992, **14**(1), 1.
9. J. Skupińska, *Chem. Rev.* 1991, **91**, 613.
10. B. Reuben and H. Wittcoff, *J. Chem. Educ.* 1988, **65**, 605.
11. E. R. Fretias and C. R. Gum, *Chem. Engng Prog.* 1979, **75**, 73.
12. Y. Chauvin, D. V. Quang, J. Gillard and J. W. Andrews, *Chem. Ind.* 1974, 375.
13. Y. Chauvin, J. Gillard, J. Leonard, P. Bonifay and J. W. Andrews, *Hydrocarbon Process.* 1982, **61**(5), 110.
14. Y. Chauvin, in *Industrial Applications of Homogeneous Catalysis* (Edited by A. Mortreux and F. Petit), pp. 177–191. D. Reidel, Dordrecht (1988).
15. S. J. Brown, L. M. Clutterbuck, A. F. Masters, J. I. Sachinidis and P. A. Tregloan, *Appl. Catal.* 1989, **48**, 1.
16. O. T. Onsager, H. Wang and U. Blindheim, *Helv. Chim. Acta* 1969, **52**, 230.
17. F. K. Smidt, L. V. Mironova, A. G. Proidakov, G. A. Kalabin, G. V. Ratovskii and T. V. Dmitieva, *Kinet. Katal.* 1978, **19**, 150.
18. J. P. Fackler, Jr. and A. F. Masters, *Inorg. Chim. Acta* 1980, **39**, 111.
19. D. F. Shriver, *The Manipulation of Air Sensitive Compounds*. McGraw-Hill, New York (1969).
20. R. D. Shalders, PhD Thesis, University of Melbourne (1992).
21. L. M. Clutterbuck, L. D. Field, G. B. Humphries, A. F. Masters and M. A. Williams, *Appl. Organomet. Chem.* 1990, **4**, 507.
22. S. J. Brown, A. F. Masters, M. Vender, J. I. Sachinidis and P. A. Tregloan, *Polyhedron* 1990, **9**, 2809.